



Contents lists available at ScienceDirect

Arabian Journal of Chemistry

journal homepage: www.ksu.edu.sa

Original article

Mechanical and dynamic mechanical behavior of 3D printed waste slate particles filled acrylonitrile butadiene styrene composites

Imtiyaz Khan^a, Neeraj Kumar^a, Mahavir Choudhary^b, Sunil Kumar^c, Tej Singh^{d,*}^a Department of Mechanical Engineering, Suresh Gyan Vihar University, Jaipur 302017, India^b Department of Mechanical Engineering, Malaviya National Institute of Technology, Jaipur, 302017, India^c Department of Nanotechnology and Advanced Materials Engineering and HMC, Sejong University, Seoul 05006, South Korea^d Savaria Institute of Technology, Faculty of Informatics, ELTE Eötvös Loránd University, Szombathely 9700, Hungary

ARTICLE INFO

Keywords:

Acrylonitrile butadiene styrene (ABS)

Waste slate particles

Fused deposition modeling

3D printing

Dynamic mechanical properties

ABSTRACT

This study analyses the feasibility of utilizing waste slate particles as a strengthening component in affordable 3D-printed composite materials to address environmental issues associated with waste management. Composite filaments were created by incorporating waste slate particles (5 %, 10 %, and 15 % by weight) into an acrylonitrile butadiene styrene (ABS) matrix and subsequently evaluated for mechanical properties. A twin-screw extruder obtained the composite filaments, while test samples were produced using a 3D printer by fused deposition modelling. The developed composites have a gradual variation in evaluated properties, about an 8 % increase in hardness, and a 40 % increase in flexural and tensile modulus was noted on the inclusion of 15 wt % of waste slate particles in the ABS matrix. The composites filled with 10 wt% and 5 wt% waste slate particles exhibited the maximum flexural strength (65.24 MPa) and tensile strength (42.11 MPa), respectively. These values were 5 % and 8 % higher than those of unfilled ABS. Furthermore, it was shown that the ABS matrix saw a decrease in elongation and impact strength as the dosage of slate particles increased. The fractured surface morphology indicated that filament breaking, filler pullout, and the creation of voids between neighbouring layers were the primary causes of material failure. The dynamic mechanical analysis (DMA) results show the reinforcing effect of slate particles by an increase of storage modulus with 13 % at 35 °C for the composite with 10 wt% slate particles and 20 % for that with 15 wt% slate particles. DMA results analyzed the composite's adhesion factor, degree of entanglement, reinforcement efficiency factor, and effectiveness factor to clarify the reinforcing mechanism of slate particles. The study determines that the most effective utilization of waste slate particles in an ABS matrix is achieved by including 10 wt%. The results of this study enhance the concept of recycling waste slate powder and reveal the potential for their utilization in several industries, including the aerospace, automotive, healthcare, and architectural sectors of 3D printing.

1. Introduction

In recent decades, the acrylonitrile–butadiene–styrene (ABS) polymer has gained popularity in engineering applications because of its excellent mechanical strength and ease of processing (Kubar et al., 2022). ABS, a thermoplastic material, is widely used in the automotive, pipeline, and household appliances industries. It combines acrylonitrile for heat and chemical resistance, butadiene for impact resistance, and styrene for processability and rigidity (Almutairi et al., 2023; Yudhanto et al., 2023). The polymer's compatibility in additive manufacturing, specifically with the fused deposition modelling (FDM) technique, has substantially increased its usage (Mwania et al., 2023). Minerals are

commonly used as fillers in ABS composites due to their low cost, un-complicated processing characteristics, and significant effect on physical, mechanical, and thermo-mechanical properties (Kuram, 2019; Madkour et al., 2021). Previous investigations thoroughly examined the impact of several minerals on ABS composites: Taghinejad et al. (2012) examined the ABS composites filled with titanium dioxide and showed how particle dispersion significantly affects their rheological properties. Tayfun et al. (2022) found that incorporating pumice into ABS improved mechanical characteristics, including increased tensile strength, impact resistance, and hardness. Pumice enhanced ABS's glass transition temperature and thermal stability. Alghadi et al. (2019) observed that adding perlite minerals to ABS enhanced tensile strength, elongation,

* Corresponding author.

E-mail addresses: mahavir.choudhary@gmail.com (M. Choudhary), sht@inf.elte.hu (T. Singh).<https://doi.org/10.1016/j.arabjc.2023.105559>

Received 28 June 2023; Accepted 12 December 2023

Available online 13 December 2023

1878-5352/© 2023 The Author(s). Published by Elsevier B.V. on behalf of King Saud University. This is an open access article under the CC BY-NC-ND license (<http://creativecommons.org/licenses/by-nc-nd/4.0/>).

and Young's modulus. Nevertheless, it resulted in a reduction in impact strength and storage modulus. Alhallak et al. (2020) investigated ABS composites with bentonite and reported improvements in tensile strength, elongation, hardness, storage modulus, and glass transition temperature. However, there was a decrease in impact strength. Osman and Atia (Osman and Atia, 2018) studied ABS composite filaments with rice straw and observed that increased rice straw content decreased strength while raising water absorption in the composite. Billah et al. (Billah et al., 2020) developed ABS composites with short-fiber reinforcement, which showed increased thermal stability, including enhanced glass transition, heat dissipation, and viscoelasticity. Zhou et al. (Zhou et al., 2020) used ethylene-methyl acrylate copolymer and nano-sodium montmorillonite as compatibilizers and fillers, respectively, to balance the bounding strength and ductility, which improve the tensile behaviour of polycarbonate/ABS FDM parts. Al-Mazrouei et al. (Al-Mazrouei et al., 2022) investigated the influence of silica dioxide on ABS composites. It was observed that higher concentrations of silica dioxide resulted in decreased tensile strength, ductility, and toughness while enhancing the elastic modulus. Doner et al. (Doner et al., 2023) examined 3D-printed hybrid thermoplastic polyurethane/ABS composites with iron particle loadings from 2.5 % to 10 % by weight. It reveals that increasing iron powder concentration by up to 5 % improved tensile strength, indentation hardness, elastic modulus, and fracture toughness. Bonda et al. (Bonda et al., 2015) investigated the influence of fly ash loading on the mechanical, thermo-mechanical performance of ABS composites. It was observed that increasing the fly ash content reduced the tensile and impact strength but increased the damping factor, tensile modulus, and storage modulus. Similarly, the blending of polymer impacts the properties of the composite, such as antibacterial, thermal, electrical, quantum, and optical (Abdelghany et al., 2019; Farea et al., 2020a, 2020b; Elashmawi et al., 2013; Zidan et al., 2016). These outcomes provide valuable information for custom material design and innovative applications in multiple industries.

The production industry is now utilizing waste materials extensively, which offers multiple benefits, including reducing pollution from waste disposal and facilitating the development of more affordable products (Singh, 2023; Lendvai, and Patnaik, 2022; Ouadrhiri et al., 2023). This strategy follows the ideas of a circular economy, which diverges from the linear model of extracting, using, and disposing of resources (Singh, 2021; Yaashikaa et al., 2022). Alternatively, it prioritizes reusing discarded materials, promoting sustainability and reducing the environmental impact (Unuofin et al., 2022; Nabgan et al., 2023; Lendvai, 2023). Slate, a naturally occurring sedimentary rock frequently used for roofing, exhibits remarkable resilience compared to alternative materials such as wood, clay tiles, or metal. However, acquiring a usable slate resulted in substantial waste, accounting for 75 % to 90 % of the total weight. This waste is typically discarded in landfills, leading to several economic, technical, social, and environmental difficulties (Campos et al., 2004; Samper et al., 2015). The waste slate materials contain significant amounts of the traditional filler components used to create polymer-based composites, such as silicon dioxide, iron oxide, aluminium oxide, calcium oxide, titanium oxide, magnesium oxide, etc. (Frías et al., 2014; Carbonell-Verdú et al., 2015). Instead of obtaining new raw materials, which can be costly, manufacturers can use waste slate material readily available at low cost or even free, resulting in economic benefits to industries. Waste slate is reported to be used in numerous applications, including cementitious material (Frías et al., 2014), manufacturing tiles (Campos et al., 2004), greywater treatment (Zipf et al., 2016), brick production (Wang et al., 2021), and automotive brake friction materials (Binda et al., 2020).

In contrast, the literature on using waste slate materials in polymeric composites is scarce. Samper et al. (Samper et al., 2015) reported that a composite based on an epoxidized linseed oil matrix with silanized waste slate fiber significantly affected the evaluated mechanical properties such as elastic modulus, flexural modulus, tensile, flexural, and impact strength. Carbonell-Verdú et al. (Carbonell-Verdú et al., 2015)

examined the influence of waste slate fiber inclusion on the mechanical and dynamic mechanical properties of high-density polyethylene composites. It was observed that with increased slate fiber dosages, the mechanical strength (tensile, impact, and flexural) and modulus (tensile, storage, and flexural) rise while elongation at break decreases. Quiles-Carrillo et al. (Quiles-Carrillo et al., 2019) investigated the effect of waste slate fiber on the mechanical and dynamic mechanical properties of polyamide 1010-based composites. Adding waste slate fiber to a polyamide 1010 matrix increased the material's Shore D hardness, tensile strength, and modulus, but it decreased its impact strength and elongation at break. For waste slate fiber loading, there was a noticeable increase in the storage modulus of polyamide 1010 and a slight increase in the glass transition temperature. Khan et al. (Khan et al., 2023) studied the impact of waste slate particles on the mechanical and thermomechanical properties of 3D printed poly(lactic acid) composites. The results indicate that an increase in the quantity of waste slate particles leads to improvements in the examined parameters, such as hardness, impact strength, storage modulus, and elastic modulus. However, the elongation at break reduces as a result.

The results obtained from previous research indicate that waste slate material can improve the mechanical and dynamic mechanical properties of polymer-based composites. This makes it a promising option for further investigation, especially in ABS matrices. Therefore, this study attempts to make a valuable addition to this expanding area by introducing an innovative method: utilizing ABS filament enhanced with waste slate particles for 3D printing applications. This study examines the mechanical and thermo-mechanical properties of ABS filaments that were 3D-printed and strengthened with 5 %, 10 %, and 15 % by-weight waste slate particles. Furthermore, it aims to assess the practicality, advantages, and economic and environmental benefits of including waste slate particles as fillers in ABS-based 3D-printed composites. The outcome of this study offers novel and valuable perspectives on the recycling of waste slate powder, proposing a unique strategy for its incorporation into various industries. The acquired information provides novel prospects for diverse applications in 3D printing, introducing revolutionary approaches in sectors including aerospace, automotive, healthcare, and architecture.

2. Experimental

2.1. Materials

In this study, waste slate particles with a density of 2.51 g/cc are gathered from local slate processing industries of Mandasaur district, Madhya Pradesh, India. The micrograph and camera images of waste slate particles are shown in Fig. 1. The slate particles are dried in the oven for 30 min to eliminate the vapors and then sieved to obtain a size of less than 20 μm for filler. The chemical composition of the used waste slate particles is listed in Table 1. The ABS granules with a density of 1.05 g/cc are procured from STALLION Enterprise International Trade Company, Rajkot (Gujarat, India).

2.2. Filament fabrication process

The complete fabrication process of filament, 3D printing of specimen and different characterization are shown in Fig. 2. The waste slate particles and ABS granules are mixed at room temperature and then compounded in a twin screw extruder from 170 °C to 230 °C. Extrusion process parameters during the compounding of ABS and waste slate particles are shown in Table 2. The compositions of ABS filament by weight of the waste slate fillers are 0, 5, 10 and 15 % and designated as ABS/SP0, ABS/SP5, ABS/SP10, and ABS/SP15, respectively. The obtained waste slate particle-filled ABS composite filament with a diameter of 1.75 mm is suitable for FDM and is then used to print 3D specimens. Adroitec Engineering Solutions (P) Ltd. FDM 3D printer prints 3D specimens, as shown in Fig. 3. The test specimens for different



Fig. 1. Waste slate particles (a) Camera image and (b) Microscopic image.

Table 1

Chemical composition (%) of waste slate particles as per IS 9749: 2007 standard.

SiO ₂	MgO	CaO	Fe ₂ O ₃	Al ₂ O ₃	Na ₂ O	K ₂ O	Loss on ignition
59.13	1.57	0.73	1.44	20.93	8.18	4.64	3.28

characterization (tensile, flexural, impact and dynamic mechanical) are fabricated per ASTM standards, as shown in Fig. 4. Five specimens are printed for each of all compositions with keeping the constant 3D printing process parameters, as shown in Table 3. The fabricated specimens are precisely measured for width and thickness. However, most of the samples possessed a dimensional accuracy of 98.5 %. A 0.4 mm nozzle diameter and other printing process parameters are shown in Table 3 considered for the assessment. The 98.5 % accuracy in

dimensions shows that the printability factors are well-controlled and optimized. It also shows the factors used to print the 3D model using developed filaments that ensure reliability and precision.

3. Measurements

Tensile characteristics (strength, elongation at break and modulus) were determined using the ASTM D638 standard. Tensile tests were

Table 2

Extrusion process parameter for filaments preparation.

Screw speed (rpm)	Temperature (°C)			
	Feed zone	Compression zone	Metering zone	Die
35	190	200	230	230

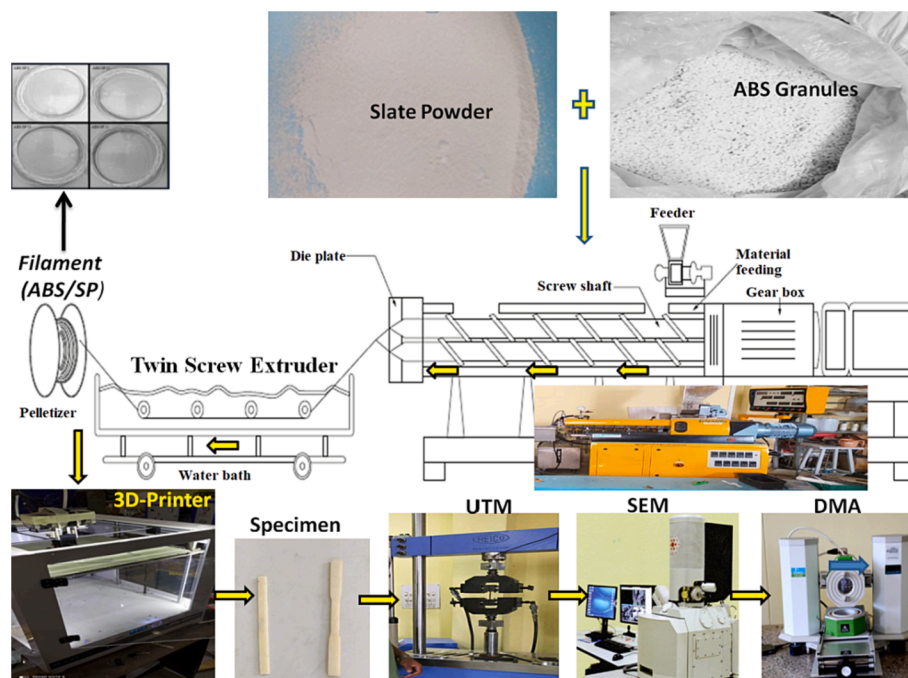


Fig. 2. Diagram of the fabrication of ABS/SP composite.

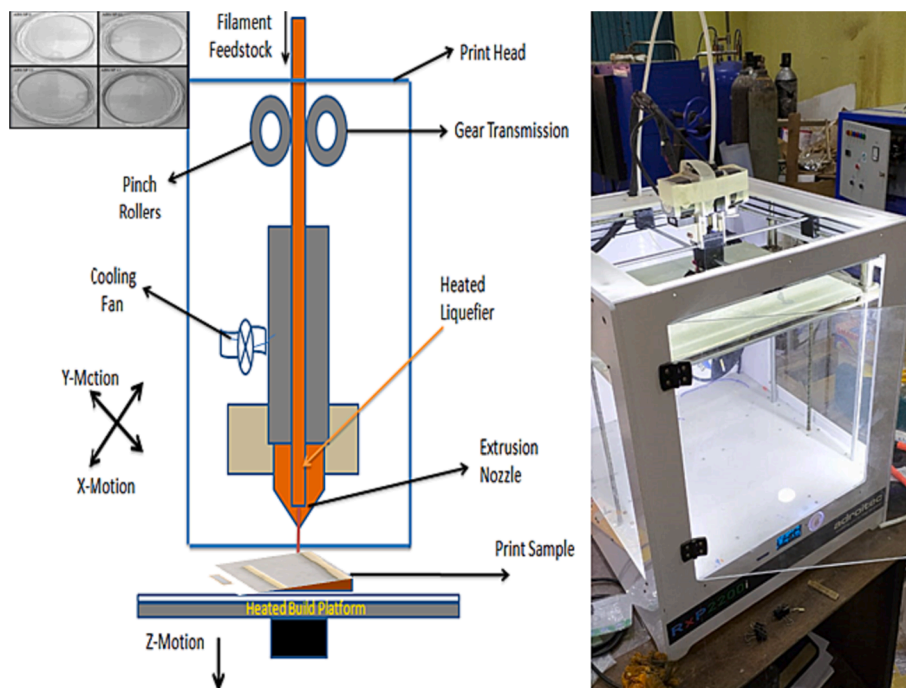


Fig. 3. FDM printing process is shown schematically.

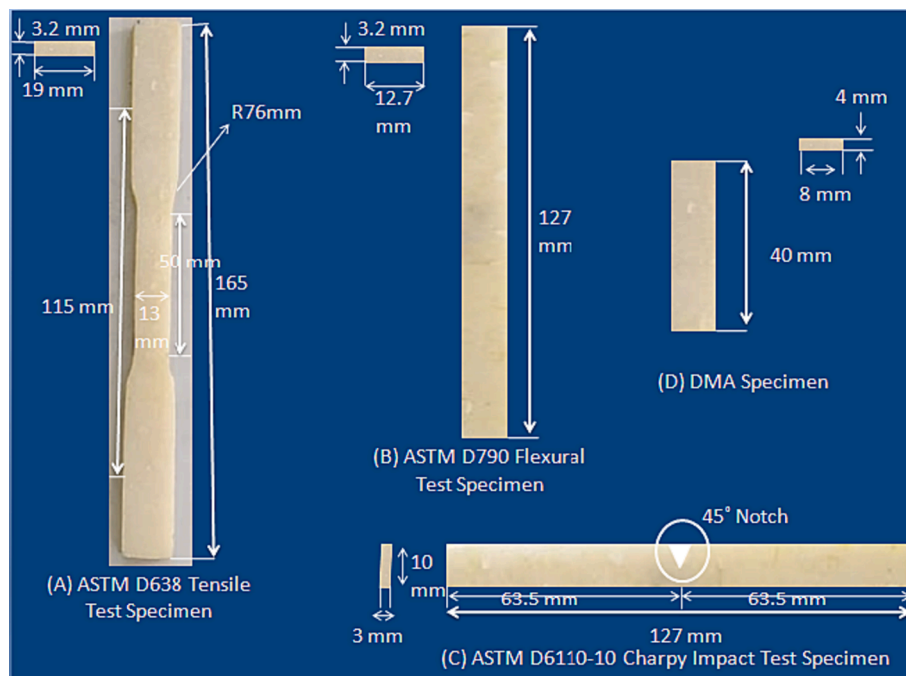


Fig. 4. Composite samples.

conducted using a servo-hydraulic universal testing machine (UTM) from HEICO (New Delhi, India) with a 2 mm per minute cross-head speed. The flexural characteristics (strength and modulus) were calculated on the same UTM machine in line with ASTM D790. Charpy impact tests were performed on 3D printed slate particles filled and unfilled ABS composite samples using an IMPACT testing machine, Instron CEAST 9050, following the standard ASTM D6110-10. Shore hardness type D was determined using a Zwick 3131 Durometer and PN-ISO 868. Fig. 4 depicts the specimens used to perform the various characterization tests specified by the ASTM standard. The statistical standard deviation was

calculated using data from five specimens of each composite sample, and the average values were utilized to depict the assessed parameters at varied slate particle loadings. The temperature-dependent viscoelastic characteristics of 3D-printed slate particle-filled and unfilled ABS composites were characterized utilizing dynamic mechanical analysis (DMA). The Perkin Elmer DMA 8000 dynamic mechanical analyzer was used to conduct the tests at 1 Hz, as specified by the ASTM D4065 standard. The samples' dimensions (Fig. 4) were 40 mm in length, 8 mm in width, and 4 mm in thickness, and the tests were conducted in three-point bending mode. Under a nitrogen atmosphere, a heating ramp was

Table 3
Formulation variable of FDM 3D printing machine.

Operation parameter of FDM	Value
Temperature (bed and nozzle)	60 °C and 230 °C
Rate of infill	100 %
Pattern of infill	Rectilinear
Angle(raster)	0°
Thickness of layer	0.1 mm
Width extrusion	0.45 mm
Speed (Printing)	45 mm/s
Shell circumference	3
Orientation(sample)	Flat

performed from 35 °C to 160 °C at 2 °C per minute. From 35 °C to 160 °C, temperature-dependent graphs for the storage modulus (E'), loss modulus (E''), and loss factor ($\tan\delta$), which is the ratio of E'' to E' , were recorded.

4. Result and discussions

4.1. Tensile properties

The tensile strength, tensile modulus, and elongation results of the investigated ABS-based composite using slate particles as filler are presented in Fig. 5. According to the data, pure ABS/SP0 has a tensile strength of 38.90 MPa. The incorporation of 5 wt% of waste slate particles into the ABS matrix caused ~3 % enhancement in the tensile strength for the ABS/SP5 composite. While for ABS/SP10 composite having 10 wt% waste slate particles, the tensile strength increased ~8 % compared to pure ABS and remained highest with 42.11 MPa. Compared to ABS/SP0 composite, a marginal decrease in tensile strength was noted for increased filler loading to 15 wt% in ABS/SP15 composite. It has been concluded that 15 wt% waste slate particles filled ABS composite (i.e. ABS/SP15) exhibits the lowest tensile strength of ~38.39 MPa. This is mostly because of filler particles' inadequate dispersion or agglomeration. This can result in poor layer adhesion and printing defects, including warping, voids, or inconsistencies, which ultimately compromise the overall strength of the 3D-printed component. Unlike the trend obtained for the tensile strength of the investigated composite, the tensile modulus values were observed to increase with increased waste slate particle loading. The lowest tensile modulus of 0.96 GPa was noted for unfilled ABS (i.e. ABS/SP0), while the inclusion of 5 wt% (i.e. ABS/SP5) and 10 wt% (i.e. ABS/SP10) waste slate particles filled composites and enhancement of ~8 % and ~26 % in tensile modulus was noted. For the composite ABS/SP15 with 15 wt% waste slate particles, the tensile modulus attained the maximum value of 1.35 GPa, almost 40 % higher than pure ABS (i.e., ABS/SP0). The improvement in modulus can be attributed to the enhanced stiffness of the waste slate particles,

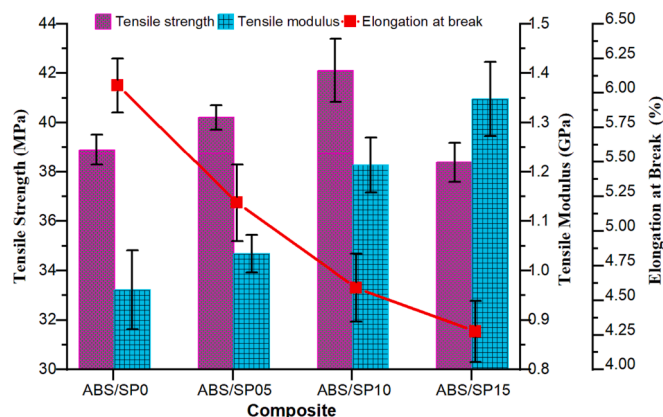


Fig. 5. Tensile test results.

which utilize the inherent hardness and strength of minerals like silicon dioxide (59.13 %), aluminum oxide (20.93 %) and iron oxide (1.44 %). This, consequently, results in an overall increase in the modulus of the composite material (Quiles-Carrillo et al., 2019; Khan et al., 2023). The results are in line with prior research that found enhanced tensile strength and modulus in various waste slate materials reinforced polymer composites. Incorporating waste slate fibers into epoxidized linseed oil (Samper et al., 2015), high-density polyethylene (Carbonell-Verdú et al., 2015), and polyamide 1010 (Quiles-Carrillo et al., 2019), as well as waste slate particles into poly(lactic acid) (Khan et al., 2023), for example, has been shown to improve the tensile strength and modulus of the resulting composites.

Furthermore, increasing the amount of waste slate particles in the ABS matrix caused a gradual fall in elongation at break. As the percentage of waste slate particles in the ABS matrix increases from 5 wt% to 15 %, the material's elongation at break decreases by 14.04 % to 29.40 %. This reduction in elongation at break was ascribed to increased stiffness of the composites with increased waste slate particle loading (Quiles-Carrillo et al., 2019; Khan et al., 2023). The inclusion of small-sized fillers of high stiffness was reported to form rigid interfaces within the polymer matrix, resulting in increased modulus and decreased composite elongation (Pedrazzoli et al., 2014; Lendvai et al., 2019). The elongation at break value of unfilled ABS (~4.27 %) steadily declined due to waste slate particle content, bottoming at ~4.27 % with 15 wt% loading for ABS/SP15 composite. This finding is consistent with research on waste slate fibers and particles in polymer composites conducted by Carbonell-Verdú et al. (Carbonell-Verdú et al., 2015), Quiles-Carrillo et al. (Quiles-Carrillo et al., 2019), and Khan et al. (Khan et al., 2023). The typical tensile curves of ABS and its composites are shown in Fig. 6. It can be observed that the higher the filler content, the lower the deformation, which might be ascribed to the poor plasticity of the waste slate particles.

Fig. 7a–f describe the scanning electron microscope (SEM) images of the fractured surface of 3D-printed tensile specimens made from ABS/SP0, ABS/SP05, ABS/SP10, and ABS/SP15 composites. This study provides an extensive visual assessment of the mode of failure, quality of adhesion, presence of defects, and overall printing quality. The provided information is significant in improving the printing parameters and ensuring the reliability of 3D-printed components in different applications. The fracture surface of ABS/SP0 tensile specimens is shown in Fig. 7a–b. The beads in the matrix–matrix chain were closely packed, but a few holes were probably caused by the polymer pulling out and breaking. With increasing filler content in the ABS matrix up to 10 wt% of waste slate powder, the tensile strength is increased due to better

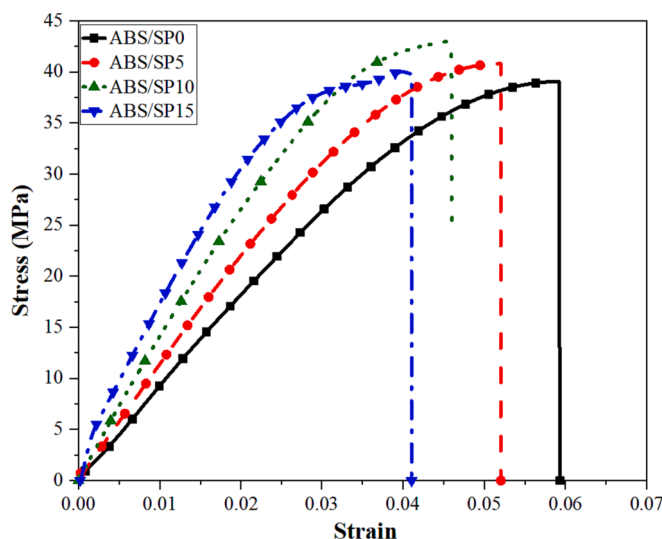


Fig. 6. Stress–strain curves.

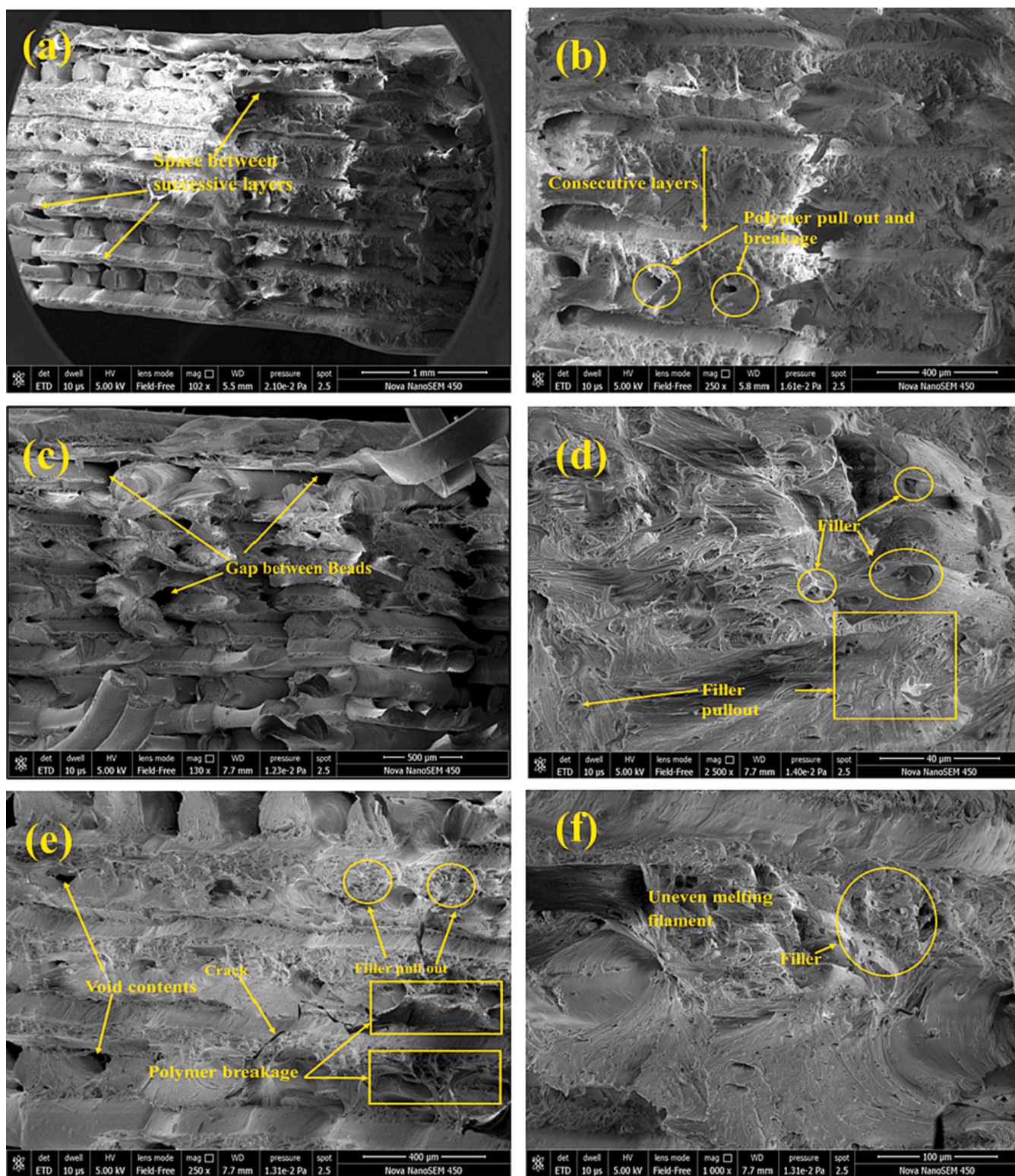


Fig. 7. SEM images of fractured surfaces.

interlayer adhesion and filler dispersion, as shown in Fig. 7c–d of the ABS/SP05 and ABS/SP10 fractured tensile specimens, respectively. When waste slate powder is added to the ABS matrix at a concentration above 10 wt%, this can lead to insufficient dispersion of the filler particles, resulting in a decrease in tensile strength. Fig. 7e–f shows the fractured surface of the ABS/SP15 tensile specimen, which reveals the failure mechanism of the tested composites, which is associated with

filament breakage and the space between the successive layers. This space acts as a void to accelerate material failure. In addition, composite failure was also associated with the removal/pull-out of waste slate particles, uneven filament melting, pull-out of waste slate particles, and poor layer adhesion (Khan et al., 2023).

4.2. Flexure properties

The evaluated ABS composites' flexural properties (strength and modulus) are compared in Fig. 8 at the different waste slate particle loadings tested (0 to 15 wt%). The flexural strength of the unfilled ABS, i.e., ABS/SP0 composite, was 62.3 MPa and showed an increase of ~5 %, including 5 wt% waste slate particles.

After exhibiting the highest value of 65.24 MPa for ABS/SP5 composites, the flexural strength decreased marginally with further slate particle loading. Compared to neat ABS, the flexural strength of ABS/SP15 composite decreased by ~3 % and remained lowest (60.15 MPa) at 15 wt% filler loading. The error bars in Fig. 8, representing the standard deviation of the ABS/SP5 and ABS/SP10 flexural strengths overlap. This suggests that the data points in both groups exhibit a comparable level of dispersion. Thus, the increase in slate powder concentration from 5 wt% to 10 wt% in the ABS matrix does not significantly affect the flexural strength. The aggregation of slate particles, which reduces the inter-phase contact surface between the ABS matrix and slate particles, may be responsible for this behaviour. Vidakis et al. (Vidakis et al., 2020) observed similar results in their research on additive-produced zinc oxide/ABS composites. The authors stated that the flexural strength of composites increases up to 5 % zinc oxide loading and decreases with greater doses. If the right amount of filler particles is added to the ABS matrix, its flexural strength can be improved. It can also be inferred from Fig. 8 that flexural modulus exhibited a steady improvement with increasing waste slate particles. For example, compared to neat ABS, i.e., ABS/SP0 composite (2.01 GPa), at 5 wt% waste slate particles loading, the increase in flexural modulus was ~8 % for ABS/SP5. At the same time, an enhancement of ~41 % in flexural modulus (2.83 ± 2 GPa) was noted for the composites having ≥ 10 wt% slate particles, i.e. ABS/SP10 and ABS/SP15. According to several pieces of research, the modulus enhancement's mechanism is higher reinforcing stiffness, which may result in an enhanced composite modulus (Pedrazzoli et al., 2014). This augmentation of flexural modulus agrees with findings on waste slate fibers/particles reinforced polymer composites published by Carbonell-Verdú et al. (Carbonell-Verdú et al., 2015) and Khan et al. (Khan et al., 2023).

4.3. Impact strength

The result of the impact strength of the waste slate particles loaded ABS composites is plotted in Fig. 9. The impact strength was shown to diminish as the waste slate particle loading increased. The impact strength of unfilled ABS, i.e., ABS/SP0 composite, is 13.25 kJ/m² and drops by ~6 % to 12.47 kJ/m² for ABS/SP5 composite, amounting to 5 wt% slate particles. However, a decrement of ~11 % in impact strength ($\sim 11.75 \pm 0.14$ kJ/m²) was noted for ABS/SP10 and ABS/SP15 composites with ≥ 10 wt% slate particle loading. Due to the low wettability of the waste slate particles in the ABS matrix, the impact strength has decreased. The aggregation of slate particles may function as stress concentration sites at higher dosages and result in cavities/voids in composite materials. When an impact force is applied, these voids encourage the growth of microcracks and hence promote crack propagation, which eventually lowers the impact strength of composites. Quiles-Carrillo et al. (Quiles-Carrillo et al., 2019) studied the

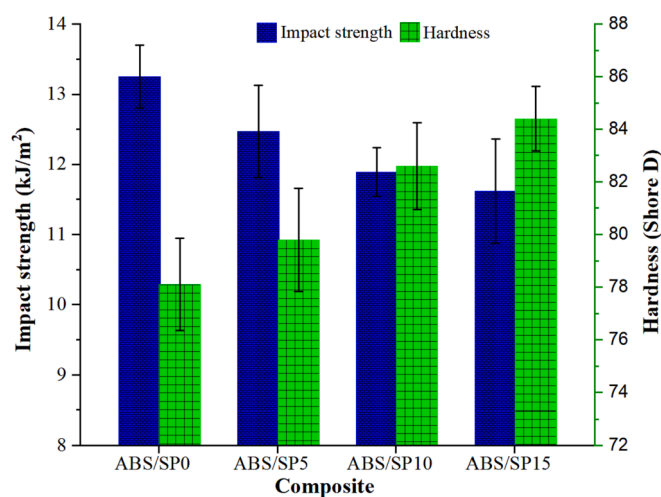


Fig. 9. Impact strength and hardness results.

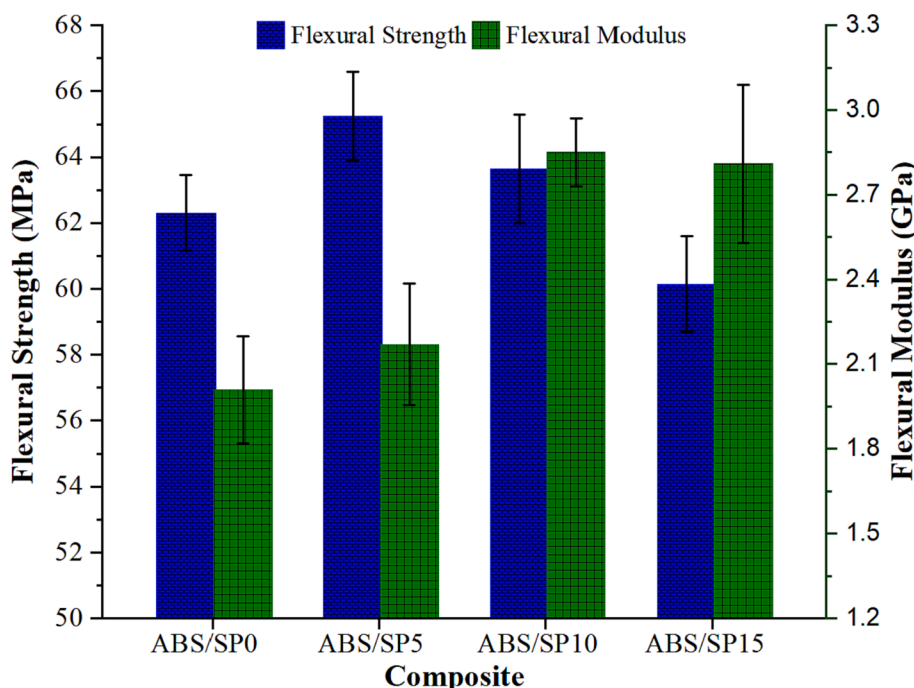


Fig. 8. Flexural test results.

mechanical and thermal performance of waste slate fibers in a bio-based polyamide 1010 matrix and likewise noticed a declining trend in impact strength. It has also been observed that the impact strength of the resulting composites is diminished when minerals such as perlite (Alghadi et al., 2019) or bentonite (Alhallak et al., 2020) are added to ABS.

4.4. Hardness

The hardness (Shore D) values of the evaluated composites filled with different waste slate particle loadings are plotted in Fig. 9. It is evident that waste slate particles filled composites showed higher hardness than the neat ABS. The lowest (78.10 Shore D) and highest (84.40 Shore D) hardness were recorded for ABS/SP0 and ABS/SP15 composites, respectively, which agreed with the literature (Lendvai et al., 2019; Khan et al., 2023). The hardness of ABS/SP5, ABS/SP10, and ABS/SP15 composites is enhanced by ~2 %, ~6%, and ~8 %, respectively, compared to unfilled ABS, i.e., ABS/SP0 composite. Fig. 9 illustrates the overlap of the error bar when comparing the harness with the progressive addition of 5 wt% slate powder in the ABS matrix at every step. This reveals that adding 5 wt% to the ABS matrix has an insignificant effect on the harness of the composite. The following consequences can be associated with increasing hardness: First, waste slate particles contain 59 % silica, which acts as a reinforcing agent. This improves the composite's overall integrity, increasing rigidity, as shown in Fig. 6. Furthermore, using hard waste slate particles restricts the mobility of polymer chains, resulting in higher plastic deformation resistance. This pattern aligns with prior research (Quiles-Carrillo et al., 2019; Khan et al., 2023), which documented a rise in the hardness of polymer composites when reinforced with waste slate fibers/particles. It has also been reported that the amalgamation of pumice mineral (Tayfun et al., 2022), bentonite mineral (Alhallak et al., 2020), iron particles (Doner et al., 2023), and zinc oxide particles (Vidakis et al., 2020) into ABS increases the hardness of the resulting composites. Table 4 compares the present study with the other reinforcement in the ABS matrix.

4.5. Dynamic mechanical analysis (DMA)

The DMA was used to determine the influence of the waste slate particle loadings on the viscoelastic performance of ABS composites. Fig. 10a shows the variation of the storage modulus (E'), Fig. 10b the loss modulus (E''), and Fig. 10c the $\tan\delta$ profile of the investigated composites as a function of temperature. As illustrated in Fig. 10a, composites exhibit three distinct behaviours based on their molecular mobility: glassy (<95 °C), glass transition (95–120 °C), or rubbery (>120 °C). Composites containing slate particles displayed greater E' values than unfilled ABS up to 120 °C, indicating the reinforcing effect of the slate particles. As the slate particle loadings were raised in composites, the mobility and deformation of the ABS matrix were reduced, leading to greater E' values. Similar results for increased E' values were noted in literature for waste slate fibers/particles reinforced polymer composites (Carbonell-Verdú et al., 2015; Quiles-Carrillo et al., 2019; Khan et al., 2023).

At 35 °C, the lowest E' of 2.11 GPa was noted for unfilled ABS (i.e. ABS/SP0) composite, while the inclusion of 5 wt% (i.e. ABS/SP5) and 10 wt% (i.e. ABS/SP10) waste slate particles filled composites and enhancement of ~8 % and ~13 % in E' was noted. For the composite ABS/SP15 with 15 wt% waste slate particles, the E' attained a maximum value of 2.53 GPa, almost 20 % higher than pure ABS (i.e., ABS/SP0) composite. This suggests that particle-shaped hard fillers like slate particles significantly affect composite elastic properties and explain the considerable tensile modulus increase. The prominent peak in the curve of E'' is a recognizable result of the 3D molecular organization of the polymer matrix. Fig. 10b shows the change in E'' with increased temperature due to adding waste slate particles to the ABS matrix. The relaxation peak, connected to the mobility of the polymer chains during

Table 4

Comparison of the additional reinforcements in ABS with the current study.

Authors	Materials	Findings
Osman and Atia, 2018	ABS-rice straw (RS) composite (0 %, 5 %, 10 %, 15 % and 20 % RS)	The incorporation of RS in ABS causes a decrease in the tensile and flexural properties of composites.
Alghadi et al., 2019	ABS filled with perlite mineral (PER) (2.5 %, 5 %, 10 %, and 15 % PER)	Up to 5 % inclusion of PER tensile strength increased. Impact strength decreased with the addition of PER.
Bonda et al., 2015	ABS with fly ash (0 %, 5 %, 7 %, 10 %, and 15 %)	Tensile strength rose with lower fly ash addition (up to 5 %) and declined with larger loading (over 5 %). Loading the fly ash increased tensile modulus while decreasing impact strength.
Alhallak et al., 2020	ABS with bentonite mineral (BNT) (5 %, 10 %, 15 % and 20 %)	The addition of BNT enhanced the hardness and tensile strength but lowered the impact strength. The results show that 15 % was the best choice for making ABS/BNT composite.
Al-Mazrouei et al., 2022	ABS with silica (0 %, 5 %, 10 % and 15 %)	As the silica loading increased from 0 % to 15 %, the tensile strength declined. At 10 %, the maximum tensile modulus was measured to be 2677.8 MPa.
Present study	ABS with slate powder (SP) (0 %, 5 %, 10 % and 15 % by weight)	At 10 % SP loading, the ABS/SP composite had a maximum tensile strength of 42.11 MPa. Adding 0 % to 15 %, SP increased the tensile modulus from 0.96GPa to 1.35GPa. Flexural strength peaked at 65.24 MPa at 5 % SP and declined with increasing loading. With the addition of SP, the ABS/SP composite became harder, but its impact strength dropped.

the change from a crystalline to an amorphous molecular structure, was given credit for the highest value of E'' (Osman and Atia, 2018). In contrast to unfilled ABS, the relaxation peaks of composites filled with slate particles are moved to higher temperatures in Fig. 10b. This suggests that the addition of stiff slate particles has reduced the flexibility of the ABS chains (Quiles-Carrillo et al., 2019; Khan et al., 2023). The highest E'' for unfilled ABS (i.e., ABS/SP0) composite was ~531 MPa at 101 °C. It shifted to a higher temperature of 104 °C for ABS/SP5, 106 °C for ABS/SP10 and 107 °C for ABS/SP15 composites with E'' values of ~768 MPa, ~970 MPa and ~1215 MPa, respectively. These results indicate that ABS composites containing slate particles are superior to unfilled ABS (i.e., ABS/SP0) composites' ability to convert mechanical energy into thermal energy (Jyoti et al., 2016).

The peak intensity difference between slate particle-filled and unfilled ABS composites was also normalized to that of an unfilled ABS composite to calculate the damping reduction (%) using the following formula (Khan et al., 2023).

$$\text{Damping reduction}(\%) = \left(1 - \frac{(\tan\delta)_c}{(\tan\delta)_m} \right) \times 100 \quad (1)$$

where $\tan\delta$ = damping factor, while subscripts m and c denote matrix and composite.

Waste slate particle-filled ABS composites showed a 4 % to 18 % damping reduction, indicating an improved ABS-slate particle contact. The damping properties of ABS composites are listed in Table 5.

The E''/E' ratio, which indicates molecular internal friction or mechanical damping in a viscoelastic configuration, is represented by the $\tan\delta$ (loss factor) (Quiles-Carrillo et al., 2019). Fig. 10c depicts the influence of waste slate particle loadings on the $\tan\delta$ for the ABS composite. The variations in the stiffness of the manufactured ABS composites were further validated by the glass transition temperature

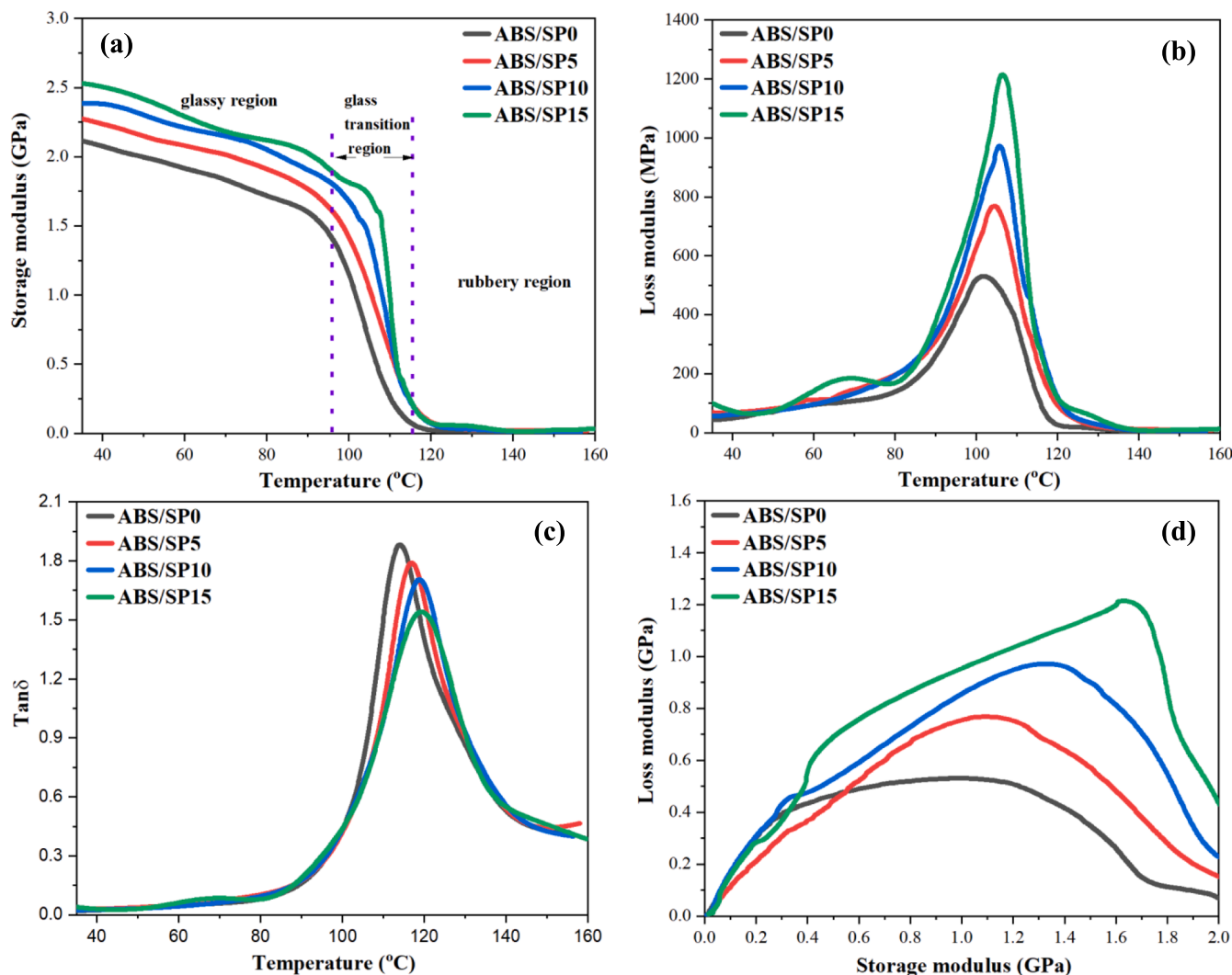


Fig. 10. (a) E' , (b) E'' , (c) $\tan\delta$, and (d) cole-cole plot.

Table 5
Damping properties of slate particles filled ABS composites.

	Composites			
	ABS/SP0	ABS/SP5	ABS/SP10	ABS/SP15
T_g ($^{\circ}\text{C}$)	114.08	116.93	118.83	119.37
Peak intensity	1.88	1.79	1.70	1.54
Damping reduction (%)	–	4.79	9.57	18.08

(T_g), which corresponds to the highest value of the $\tan\delta$ versus temperature curve. As seen in Fig. 11c, adding waste slate particles pushes the $\tan\delta$ peak to higher temperatures and reduces the peak intensity. The peak intensity for the ABS/SP0 composite was 1.88 and was noted to decrease to 1.79, 1.70, and 1.54 for ABS/SP5, ABS/SP10, and ABS/SP15 composites, respectively, as shown in Table 4. The T_g for unfilled ABS (i.e., ABS/SP0) composite was 114.09 $^{\circ}\text{C}$ and found to shift towards higher temperatures of 116.93 $^{\circ}\text{C}$, 118.83 $^{\circ}\text{C}$, and 119.37 $^{\circ}\text{C}$, respectively, for ABS/SP5, ABS/SP10, and ABS/SP15 composites. This suggests that incorporating waste slate particles in a greater quantity significantly restricts the mobility of the ABS chains. Similar results for T_g enhancement of polymer composites with waste slate fibers/particles were reported in the literature (Quiles-Carrillo et al., 2019; Khan et al., 2023). It has also been observed that the T_g of the resulting composites is shifted to higher temperatures when minerals such as pumice (Tayfun et al.,

2022) or bentonite (Alhallak et al., 2020) are added to ABS.

The Cole-Cole analysis can examine how the structural properties change when slate particles are added to a cross-linked polymer matrix. For this purpose, E' vs E'' plots have been created to compare slate-particle-filled ABS composites with unfilled ABS. These plots are displayed in Fig. 10d. The semi-circular shape of cole-cole plots represents homogeneous systems. In contrast, two-phase systems show an imperfect semicircle (elliptical path) (Jyoti et al., 2016). The semi-circular form of the unfilled ABS, i.e., ABS/SP0 composite (Fig. 10d), shows the shape of the semicircle, which turns towards an imperfect semi-circular shape with increased slate particles loading curve owing to a two-phase system. The shape of the curves thus indicates strong adhesion among the filler and matrix material (Jyoti et al., 2016; Pandey et al., 2016). To clarify the reinforcing mechanism of waste slate particles and the adhesion at the interface, four factors, namely the adhesion factor (A_F), reinforcement efficiency factor (RE_F), degree of entanglement (E_d), and effectiveness factor (ϵ_F), were used (Hejna et al., 2015; Jyoti et al., 2016; Pandey et al., 2016; Jyoti and Arya, 2020).

4.5.1. Effectiveness factor (ϵ_F)

The effectiveness of slate particles as reinforcing filler for the ABS matrix was determined by " ϵ_F " using the following equation (Jyoti and Arya, 2020):

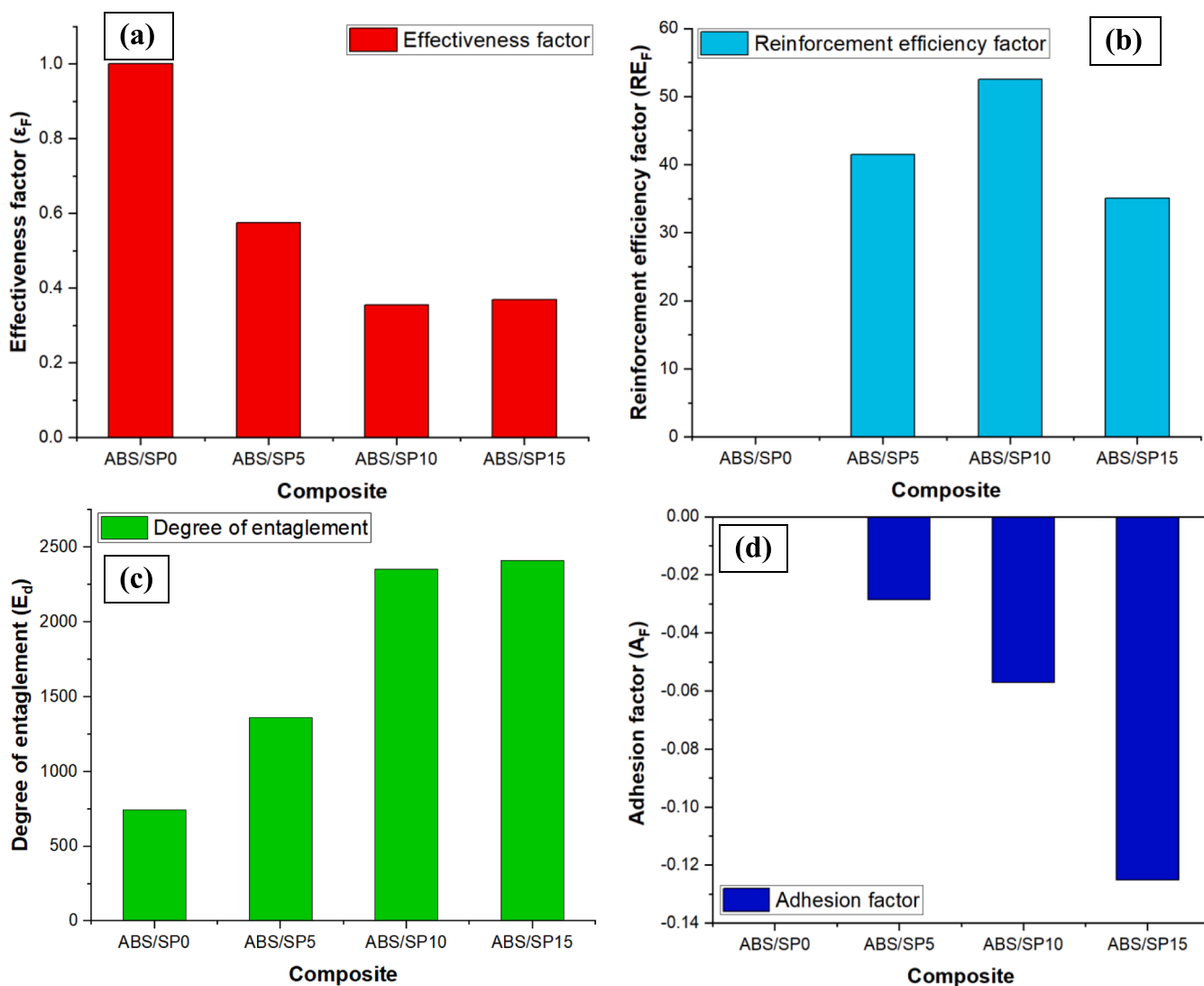


Fig. 11. Results of various factors (a) ϵ_F , (b) RE_F , (c) E_d , and (d) A_F .

$$\epsilon_F = \frac{(E'_{GR}/E'_{RR})_{composite}}{(E'_{GR}/E'_{RR})_{matrix}} \quad (2)$$

where, E'_{RR} and E'_{GR} are the E' values for the ABS matrix and composite in the rubbery and glassy regions. For E'_{GR} and E'_{RR} , the E' values at 60 °C and 130 °C were utilized. The ϵ_F value emphasizes the role of slate particles in the transition from the glassy to the rubbery state, with a lower value indicating more reinforcing efficiency. As shown in Fig. 11a, lower ϵ_F values (0.34 ± 0.01) were found for greater slate particle concentrations (≥ 10 wt%) in the ABS/SP10 and ABS/SP15 composites, indicating that slate particle content increased reinforcing effectiveness. More slate particles in ABS resulted in improved particle–matrix interactions and greater particle–particle contacts, increasing stress transfer between particles and matrix, hence reinforcing ability.

4.5.2. Reinforcement efficiency factor (RE_F)

DMA may also be used to retrieve information about RE_F in addition to the ϵ_F value. When the effect of filler fractional addition to polymeric composites is taken into account, the RE_F value provides a rough estimate of filler matrix bonding. The following formula is used to determine RE_F (Jyoti et al., 2016):

$$RE_F = \frac{1}{V_F} \left(\frac{E'_c}{E'_m} - 1 \right) \quad (3)$$

where E' is the storage modulus, subscripts m and c denote matrix and composite, while V_F is the slate particles volume fraction.

Fig. 11b depicts the RE_F plot for the unfilled and slate particles-filled ABS composites. The RE_F shows a low value for ABS/SP5 composites with 5 wt% slate particles and a high value for ABS/SP10 composites with 10 wt% slate particles. The reinforcing efficiency of ABS/SP15 composite is reduced by including 15 wt% slate particles, implying that RE_F is highly dependent on filler concentration and that better dispersion has been achieved for composites containing 10 wt% slate particles. With 10 wt% slate particle content, the obtained RE_F corresponds with the composite's higher tensile and flexural strength.

4.5.3. Degree of entanglement (E_d)

The E' acquired by DMA has also been used to determine the E_d between the filler and polymer in the polymeric composite. For the purpose of determining E_d , the following equation has been considered (Jyoti et al., 2016; Pandey et al., 2016; Jyoti and Arya, 2020):

$$E_d = \frac{E'}{6R_u T} \quad (4)$$

where, E' = storage modulus, T = temperature, R_u = universal gas constant.

The variation in E_d for ABS with and without slate particle filling, estimated at 90 °C, is shown in Fig. 11c. It has been noted that E_d rises when the ABS composites' slate particle content rises. The E_d exhibits some improvement over ABS/SP0 at smaller loadings (5 wt%) of slate particles for ABS/SP5 composite. The likelihood of contact among slate particles rises noticeably as filler particle concentration rises; this may diminish E_d , but growing entanglement behaviour in nature suggests less interaction between filler particles. The higher storage and tensile modulus of composites with higher content of slate particles is consistent with the observed E_d trend.

4.5.4. Adhesion factor (A_F)

The efficiency of reinforcement is significantly affected by the filler-matrix contact. The mechanical characteristics of composites are profoundly affected by the adhesion at the interface between the ABS and the slate particles, which permits the passage of load from the matrix to the filler particles. A robust interface is formed if the matrix and slate particles are well-mixed; otherwise, the contact is weak. The A_F was calculated using the following equation to assess the interface parameters (Hejna et al., 2015; Jyoti and Arya, 2020):

$$A_F + 1 = \frac{\tan\delta_c}{\tan\delta_m} \left(\frac{1}{1 - V_F} \right) \quad (5)$$

where $\tan\delta$ = damping factor, V_F = slate particles volume fraction, while subscripts m and c denote matrix and composite.

As shown in Fig. 11d, A_F reduced with increased slate particle loading, indicating improved interfacial contact. The composites with 15 wt% slate particles had the lowest A_F value, demonstrating improved surface adhesion with increased slate particle concentration. However, the differences in peak height and the gradual shift of T_g towards higher temperatures seen by DMA for slate particle-filled ABS composites compared to unfilled ABS imply improved interface adhesion. The increased tensile modulus and E' values of the ABS matrix with increasing slate particle loadings, as depicted in Fig. 5 and Fig. 10a, provide more evidence to support this conclusion.

5. Conclusions

This paper introduces a novel kind of 3D-printed composite material that incorporates waste slate particles into acrylonitrile butadiene styrene (ABS) using a twin-screw extruder. The study explores the effect of adding waste slate particles of different weights (5 %, 10 %, and 15 %) to unfilled ABS composites. The investigation is focused on the mechanical and thermo-mechanical behaviour of 3D-printed SP-filled and unfilled ABS composite samples. The results reveal that incorporating waste slate particles at a maximum weight percentage of 15 % increases hardness by 8 % and tensile and flexural modulus by 40 %. Loadings of waste slate particles, on the other hand, result in a reduction in impact strength. The dynamic mechanical analysis reveals that adding waste slate particles as a partial substitute for ABS led to a significant increase in the storage and loss modulus of ABS composites and a modest rise in glass transition temperature. The highest gain of storage modulus was noticed in the glassy region for 15 wt% waste slate particles filled composite. The study of the composite's adhesion factor, degree of entanglement, reinforcement efficiency factor, and effectiveness factor concluded that the most effective utilization of waste slate particles in an ABS matrix is achieved by including 10 wt%. This configuration results in an approximate 8 % increase in tensile strength, a 26 % increase in tensile modulus, a 6 % increase in hardness, a 41 % increase in flexural modulus, a 13 % increase in storage modulus, and an increase of roughly 5 °C in glass transition temperature compared to unfilled ABS. The study emphasizes that appropriately utilizing the waste slate particles leads to enhanced strength and rigidity while maintaining thermal stability. These findings

are crucial in informing the development of advanced 3D-printed polymer composites for specific applications such as structural elements, automotive components, and consumer goods. Furthermore, future research in this field may concentrate on optimizing the addition of waste slate particles for specific purposes, examining the composite materials' long-term durability and environmental consequences, and exploring additional developments in eco-friendly and affordable filler materials for 3D printing. These efforts would contribute to the advancement of sustainable additive manufacturing techniques.

Declaration of competing interest

The authors declare that they have no known competing financial interests or personal relationships that could have appeared to influence the work reported in this paper.

References

- Abdelghany, A.M., Meikhaail, M.S., Asker, N., 2019. Synthesis and structural-biological correlation of PVC/PVAc polymer blends. *J. Mater. Res. Technol.* 8 (5), 3908–3916.
- Alghadi, A.M., Tirkes, S., Tayfun, U., 2019. Mechanical, thermo-mechanical and morphological characterization of ABS based composites loaded with perlite mineral. *Mater. Res. Express* 7, 015301.
- Alhallaq, L.M., Tirkes, S., Tayfun, U., 2020. Mechanical, thermal, melt-flow and morphological characterizations of bentonite-filled ABS copolymer. *Rapid Prototyp. J.* 26, 1305–1312.
- Al-Mazrouei, N., Ismail, A., Ahmed, W., Al-Marzouqi, A.H., 2022. ABS/silicon dioxide micro particulate composite from 3D printing polymeric waste. *Polymers* 14 (2022), 509.
- Almutairi, M.D., Mascarenhas, T.A., Alnahdi, S.S., He, F., Khan, M.A., 2023. Modal response of hybrid raster orientation on material extrusion printed acrylonitrile butadiene styrene and polyethylene terephthalate glycol under thermo-mechanical loads. *Polym. Test.* 120, 107953.
- Billah, K.M.M., Lorenzana, F.A.R., Martinez, N.L., Wicker, R.B., Espalin, D., 2020. Thermomechanical characterization of short carbon fiber and short glass fiber-reinforced ABS used in large format additive manufacturing. *Addit. Manuf.* 35, 101299.
- Binda, F.F., Oliveira, V.A., Fortulan, C.A., Palhares, L.B., Santos, C.G., 2020. Friction elements based on phenolic resin and slate powder. *J. Mater. Res. Technol.* 9, 3378–3383.
- Bonda, S., Mohanty, S., Nayak, S.K., 2015. Evaluation of properties of industrial waste filled polymer composites for automobile applications. *Mater. Sci. Technol.* 31, 996–1006.
- Campos, M., Velasco, F., Martínez, M.A., Torralba, J.M., 2004. Recovered slate waste as raw material for manufacturing sintered structural tiles. *J. Eur. Ceram. Soc.* 24, 811–819.
- Carbonell-Verdú, A., García-García, D., Jordá, A., Samper, M.D., Balart, R., 2015. Development of slate fiber reinforced high density polyethylene composites for injection molding. *Compos. B Eng.* 69, 460–466.
- Doner, S., Paswan, R., Das, S., 2023. The influence of metallic particulate inclusions on the mechanical and thermal performance of 3D printable acrylonitrile-butadiene-styrene/thermoplastic polyurethane fused polymer blends. *Mater. Today Commun.* 35, 106111.
- Elashmawi, I.S., Abdelghany, A.M., Hakeem, N.A., 2013. Quantum confinement effect of CdS nanoparticles dispersed within PVP/PVA nanocomposites. *J. Mater. Sci. Mater. Electron.* 24, 2956–2961.
- Farea, M.O., Abdelghany, A.M., Meikhaail, M.S., Oraby, A.H., 2020a. Effect of cesium bromide on the structural, optical, thermal and electrical properties of polyvinyl alcohol and polyethylene oxide. *J. Mater. Res. Technol.* 9 (2), 1530–1538.
- Farea, M.O., Abdelghany, A.M., Meikhaail, M.S., Oraby, A.H., 2020b. Effect of cesium bromide on the structural, optical, thermal and electrical properties of polyvinyl alcohol and polyethylene oxide. *J. Mater. Res. Technol.* 9 (2), 1530–1538.
- Frias, M., Villa, R.V., García, R., Soto, I., Medina, C., Rojas, M.I.S., 2014. Scientific and technical aspects of blended cement matrices containing activated waste slates. *Cem. Concr. Compos.* 48, 19–25.
- Hejna, A., Formela, K., Saeb, M.R., 2015. Processing, mechanical and thermal behavior assessments of polycaprolactone/agricultural wastes biocomposites. *Ind. Crop. Prod.* 76, 725–733.
- Jyoti, J., Arya, A.K., 2020. EMI shielding and dynamic mechanical analysis of graphene oxide-carbon nanotube-acrylonitrile butadiene styrene hybrid composites. *Polym. Test.* 91, 106839.
- Jyoti, J., Singh, B.P., Arya, A.K., Dhakate, S.R., 2016. Dynamic mechanical properties of multiwall carbon nanotube reinforced ABS composites and their correlation with entanglement density, adhesion, reinforcement and C factor. *RSC Adv.* 6, 3997–4006.
- Khan, I., Kumar, N., Yadav, J.S., Choudhary, M., Chauhan, A., Singh, T., 2023. Utilization of waste slate powder in poly(lactic acid) based composite for 3D printer filament. *J. Mater. Res. Technol.* 24, 703–714.
- Kubar, A.A., Jin, N., Cui, Y., Hu, X., Qian, J., Zan, X., Zhang, C., Zhu, F., Kumar, S., Huo, S., 2022. Magnetic/electric field intervention on oil-rich filamentous algae

- production in the application of acrylonitrile butadiene styrene based wastewater treatment. *Bioresour. Technol.* 356, 127272.
- Kuram, E., 2019. Hybridization effect of talc/glass fiber as a filler in polycarbonate/acrylonitrile-butadiene-styrene composites. *Compos. B Eng.* 173, 106954.
- Lendvai, L., 2023. Lignocellulosic agro-residue/poly(lactic acid) (PLA) biocomposites: rapeseed straw as a sustainable filler. *Cleaner Mater.* 9, 100196.
- Lendvai, L., Patnaik, A., 2022. The effect of coupling agent on the mechanical properties of injection molded polypropylene/wheat straw composites. *Acta Technica Jaurinensis* 15, 232–238.
- Lendvai, L., Sajó, I., Karger-Kocsis, J., 2019. Effect of storage time on the structure and mechanical properties of starch/bentonite nanocomposites. *Starch - Stärke* 71, 1800123.
- Madkour, S.A., Tirkes, S., Tayfun, U., 2021. Development of barite-filled acrylonitrile butadiene styrene composites: mechanical, thermal, melt-flow and morphological characterizations. *Appl. Surf. Sci. Adv.* 3, 100042.
- Mwania, F.M., Maringa, M., Nsengimana, J., 2023. Investigating the effect of process parameters on the degree of fusion of two adjacent tracks produced through fused deposition modelling of acrylonitrile butadiene styrene. *Polym. Test.* 121, 107981.
- Nabgan, W., Ikram, M., Alhassan, M., Owgi, A.H.K., Tran, T.V., Parashuram, L., Nordin, A.H., Djellabi, R., Jalil, A.A., Medina, F., Nordin, M.L., 2023. Bibliometric analysis and an overview of the application of the non-precious materials for pyrolysis reaction of plastic waste. *Arab. J. Chem.* 16, 104717.
- Osman, M.A., Atia, M.R.A., 2018. Investigation of ABS-rice straw composite feedstock filament for FDM. *Rapid Prototyp. J.* 24, 1067–1075.
- Ouadrhiri, F.E., Saleh, E.A.M., Husain, K., Adachi, A., Hmamou, A., Hassan, I., Moharam, M.M., Lahkimi, A., 2023. Acid assisted-hydrothermal carbonization of solid waste from essential oils industry: Optimization using I-optimal experimental design and removal dye application. *Arab. J. Chem.* 16, 104872.
- Pandey, A.K., Kumar, R., Kachhavah, V.S., Kar, K.K., 2016. Mechanical and thermal behaviours of graphite flake reinforced acrylonitrile butadiene styrene composites and their correlation with entanglement density, adhesion, reinforcement and C factor. *RSC Adv.* 6, 50559–50571.
- Pedrazzoli, D., Khumalo, V.M., Karger-Kocsis, J., Pegoretti, A., 2014. Thermal, viscoelastic and mechanical behavior of polypropylene with synthetic boehmite alumina nanoparticles. *Polym. Test.* 35, 92–100.
- Quiles-Carrillo, L., Boronat, T., Montanes, N., Balart, R., Torres-Giner, S., 2019. Injection-molded parts of fully bio-based polyamide 1010 strengthened with waste derived slate fibers pretreated with glycidyl- and amino-silane coupling agents. *Polym. Test.* 77, 105875.
- Samper, M.D., Petrucci, R., Sánchez-Nacher, L., Balart, R., Kenny, J.M., 2015. New environmentally friendly composite laminates with epoxidized linseed oil (ELO) and slate fiber fabrics. *Compos. B Eng.* 71, 203–209.
- Singh, T., 2021. Utilization of cement bypass dust in the development of sustainable automotive brake friction composite materials. *Arab. J. Chem.* 14, 103324.
- Singh, T., 2023. Comparative performance of barium sulphate and cement by-pass dust on tribological properties of automotive brake friction composites. *Alex. Eng. J.* 72, 339–349.
- Taghinejad, S.F., Behrouzi, M., Asiaban, S., 2012. Investigation of the rheological behavior of titanium dioxide pigmented acrylonitrile-butadiene-styrene polymer. *J. Appl. Polym. Sci.* 124, 2016–2021.
- Tayfun, Ü., Tirkes, S., Doğan, M., Tirkes, S., Zahmakıran, M., 2022. Comparative performance study of acidic pumice and basic pumice inclusions for acrylonitrile-butadiene-styrene-based composite filaments. *Printing Additive Manuf.* <https://doi.org/10.1089/3dp.2022.0228>.
- Unuofin, J.O., Moloantoa, K.M., Khetsha, Z.P., 2022. The biobleaching potential of laccase produced from mandarin peelings: Impetus for a circular bio-based economy in textile biofinishing. *Arab. J. Chem.* 15, 104305.
- Vidakis, N., Petousis, M., Maniadi, A., Koudoumas, E., Kenanakis, G., Romanitan, C., Tutunaru, O., Suche, M., Kechagias, J., 2020. The mechanical and physical properties of 3D-printed materials composed of ABS-ZnO nanocomposites and ABS-ZnO microcomposites. *Micromachines* 11, 615.
- Wang, W., Gan, Y., Kang, X., 2021. Synthesis and characterization of sustainable eco-friendly unburned bricks from slate tailings. *J. Mater. Res. Technol.* 14, 1697–1708.
- Yaashikaa, P.R., Kumar, P.S., Varjani, S., 2022. Valorization of agro-industrial wastes for biorefinery process and circular bioeconomy: a critical review. *Bioresour. Technol.* 343, 126126.
- Yudhanto, A., Li, X., Tao, R., Melentiev, R., Lubineau, G., 2023. Identifying adhesion characteristics of metal-polymer interfaces: recent advances in the case of electroplated acrylonitrile butadiene styrene. *Mater. Today Commun.* 35, 106218.
- Zhou, Y.-G., Zou, J.-R., Wu, H.-H., Xu, B.-P., 2020. Balance between bonding and deposition during fused deposition modeling of polycarbonate and acrylonitrile-butadiene-styrene composites. *Polym. Compos.* 41, 60–72.
- Zidan, H.M., El-Ghamaz, N.A., Abdelghany, A.M., Lotfy, A., 2016. Structural and electrical properties of PVA/PVP blend doped with methylene blue dye. *Int. J. Electrochem. Sci.* 11, 9041–9056.
- Zipf, M.S., Pinheiro, I.G., Conegero, M.G., 2016. Simplified greywater treatment systems: slow filters of sand and slate waste followed by granular activated carbon. *J. Environ. Manage.* 176, 119–127.